






## Investigation of the plasma column evolution and dynamics in the PW-7 plasma accelerator

A.B. Tazhen\* , M.K. Dosbolayev , Zh.B. Igibaev ,  
A.U. Utegenov  and T.S. Ramazanov 

NNLOT, Al-Farabi Kazakh National University, Almaty, Kazakhstan

\*e-mail: Tazhen.Aigerim.B@gmail.com

(Received January 27, 2023; received in revised form March 18, 2023; accepted April 23, 2023)

In this paper the results of measurements of the azimuthal component distribution of the plasma column magnetic field in the coaxial plasma accelerator PW-7 are presented. Registration of the magnetic field was performed by the magnetic probe method. The objective of the work is to investigate the plasma column dynamics and temporal evolution distribution by the magnetic field. It has been revealed that by using a dielectric (quartz) tube limiting the plasma column, the escape of charged particles from the discharge onto the walls of the vacuum chamber can be avoided. Through the use of a dielectric tube, the redistribution of the plasma column current in the accelerator led to a change in the shape of the probe signals. In addition, the plasma velocity was measured by the time of the plasma column front, passing between the bottom of the coaxial electrode and probe measuring system. Using a rectangular screen composed of ferromagnetic material provided magnetic shielding from the quasi-static magnetic fields of the plasma jumper between the electrodes. These results allowed investigating the major peculiarities of the complex behavior of the plasma column. The main objectives of investigations at the PW-7 facility include a detailed analysis of the probe system operation, studying the effects of different discharge scenarios on the magnetic probe signals.

**Key words:** coaxial plasma accelerator, discharge current, plasma column evolution, plasma column dynamics, intrinsic magnetic field of the plasma column.

**PACS numbers:** 29.17.+w; 07.07.Df.

### 1 Introduction

Electromagnetic pulsed plasma accelerators with intrinsic magnetic field are potential sources of high-energy plasma fluxes. These units have been investigated for a wide range of applications over the past several decades. Astrophysical studies and studies of the interaction of plasma with the surface are highlighted [1, 2].

The first electromagnetic pulsed plasma accelerators were railguns. Later, they were modified to coaxial geometry. Due to their high output parameters (plasma flux density, energy, and velocity), simple design, and low cost, coaxial accelerators have been successfully utilized for simulating plasma heat fluxes that are expected to be encountered in ITER [3-6]. It is known that the plasma fluxes leads to the «breakdown erosion» of first wall materials the fusion reactor. Current studies reveal that the erosion represents a real and serious problem for fusion reactors [7-9].

The design of coaxial pulsed plasma accelerators consists of storage capacitors connected to a coaxial electrode system. The processes occurring in such systems are divided into several phases: i. initiation of a powerful electric discharge (formation of plasma jumper between electrodes); ii. development and acceleration of the current sheet in inter-electrode space, iii. compression of the current sheet outside the electrode system with the formation of dense plasma column.

To reach the high efficiency of plasma treatment and to achieve desired effect the certain conditions of the irradiation of the target with the plasma flux generated by the accelerator must be fulfilled [10-12]. One condition is that the plasma flux should be completely concentrated on the surface and interact with the entire surface uniformly. Homogeneous distribution of the plasma flux on the surface behind the electrode system is characterized by its specific structure. The structure of the plasma flux is specified in the phases of plasma formation and

acceleration. There are many mathematical models that describe the dynamics of plasma flow in coaxial plasma accelerators [13-15]. Unfortunately, there is no experimental data that can provide direct confirmation of the theoretical results. Furthermore, the issue of the plasma flux dynamics in coaxial plasma accelerators still has no definite interpretation and requires supplementary, more thorough studies.

The present work is devoted to the experimental investigation of the plasma flux in the PW-7 coaxial plasma accelerator by using a system of magnetic probes [16-18] and extends the work using magnetic probes, the results of which are described in [19].

## 2 Experimental part

The scheme of the PW-7 coaxial plasma accelerator is shown in Figure 1. The main component of the plasma accelerator is the system of electrodes (*SE*). The electrodes are made of copper. The diameter and length of the central electrode is

5.5 cm and 33 cm and the outer electrode is 10.8 cm and 35 cm. The accelerator is powered by low-inductive KPIMK-8-288 storage capacitors (*C*) with a total capacitance of 1.4 mF. The capacitors are charged from the high voltage power supply (*PS*) to a maximum voltage up to 8 kV. The accelerator is remotely controlled by a separate control unit (*K*). The energy stored in the capacitor battery is transferred to the electrode system through a vacuum arrester. The electrodes are located inside the discharge chamber. On the side walls of the discharge chamber have several observation windows (*M*). Before the experiments, the discharge chamber is pumped by vacuum pump (*VP*) to a pressure of  $10^{-3}$  Torr. The physical principle involved in plasma acceleration is that the plasma is accelerated by an electrodynamic force arising from the interaction of the current in the plasma jumper with intrinsic magnetic field. The duration of discharge in this facility can reach 300  $\mu$ s, and a maximum discharge current of  $\sim 80$  kA can be obtained at a voltage of 5 kV [20].

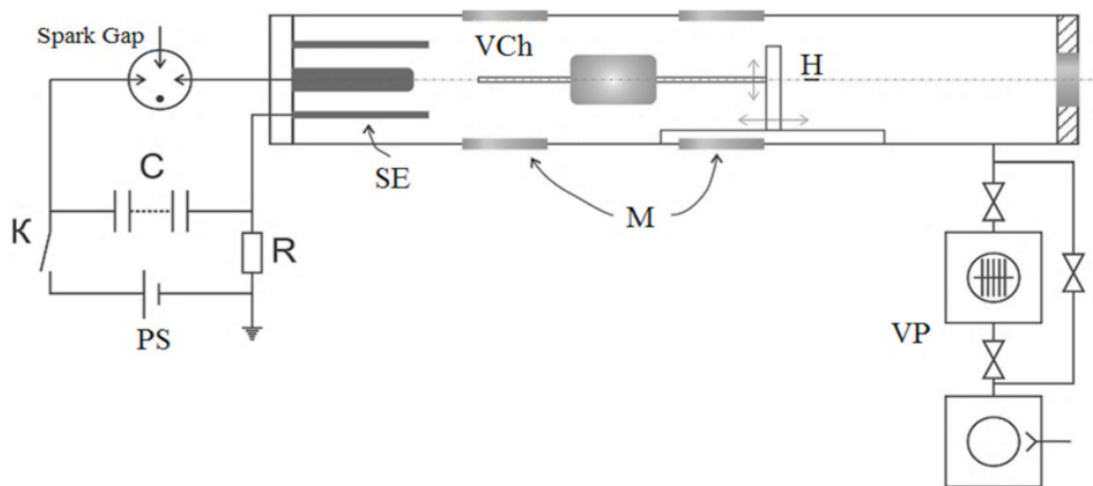


**Figure 1** – PW-7 coaxial plasma accelerator

In this work, to measure the azimuthal component of the magnetic field of the plasma cord a measuring system consisting of four magnetic probes was used, which was located at a distance of 23 cm from the edge of the electrode system (Figure 2) [21].

The use of four magnetic probes simultaneously made it possible to obtain a spatial distribution of the azimuthal magnetic field. It should be noted that the use of several probes is necessary to obtain a complete field distribution. However, due to the limited measuring channels of the oscilloscope (Lecroy Wavejet 354A digital four-channel), only four probes

were used in this work. The characteristics of the magnetic probes are as follows: the number of turns is 7, the diameter of the coils is 2.29 mm. A screen of ferromagnetic material was used to magnetically shield the probes from the quasi-static magnetic fields of the plasma jumper in the gap between the electrodes. The calibration was carried out in a homogeneous magnetic field generated in the center of the multilayer coil. The magnitude of the magnetic field was measured with a Hall sensor. The results obtained from the two magnetic sensors reasonably matches.

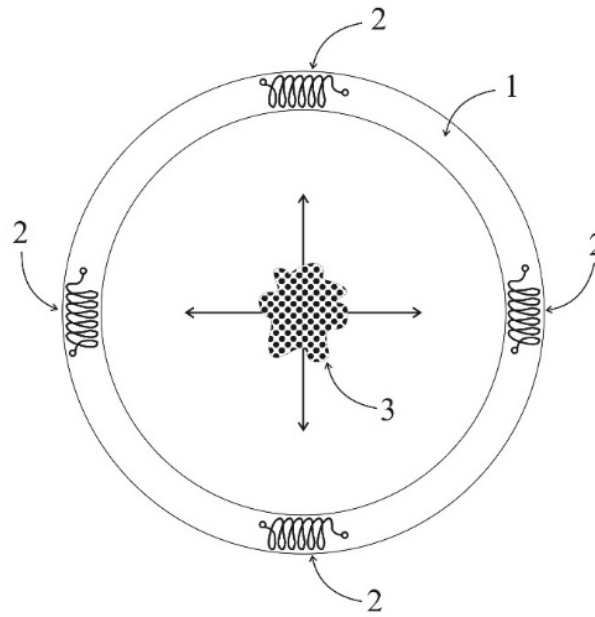


**Figure 2** – System for measuring of the plasma column azimuthal magnetic field. 1 – the frame on which the magnetic probes were attached, 2 – magnetic probes, 3 – cross-section of the plasma column (flux)

### 3 Results and Discussion

The discharge current oscillogram ( $I_d$ ) and the signals from the three magnetic probes ( $B_\varphi$ ) are shown in Figure 3. The signal recorded by the Rogowski coil [22] at the beginning indicates the occurrence

of the plasma jumper between the high-voltage electrodes. It appears near the insulating wall inside of the electrode system. In addition, high-frequency fluctuations of signals (electromagnetic noises) have been detected at that moment corresponds to the time of formation of the plasma jumper ( $t_0$ ).

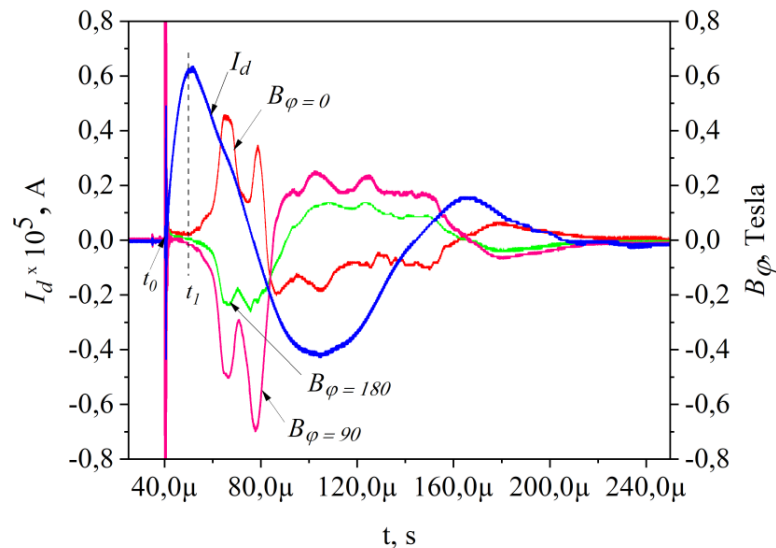


**Figure 3** – The discharge current and plasma column azimuthal magnetic field waveforms.  $U = 4$  kV,  $p = 40$  mTorr

The large radial currents flow through the plasma column. Consequently, these currents create strong magnetic fields in space. However, at this moment, the magnetic probes placed away from the electrode system do not sense magnetic flux, since the sensitivity of the magnetic probes is limited due to external screening. As can be seen in Figure 3, the current in the magnetic probes is induced about  $10 \mu\text{s}$  after the occurrence of the plasma jumper ( $t_j$ ). As it is indicated earlier, the system of magnetic probes is placed from the edge of the electrode system at a distance of 23 cm, therefore the velocity of the plasma flux can be evaluated. Correspondingly, it was approximately  $v \sim 53 \text{ km/s}$  if the distance is considered from the bottom of the electrode system.

The waveforms of the magnetic field obtained from the four probes are shown in Figure 4. The probes

were placed around the contour of a single frame at an angle of  $90^\circ$  (Figure 2). The frame is arranged perpendicular to the direction of the plasma flux. The opposite magnetic probes are spaced at a distance of 10 cm away from each other. In accordance with the B vector circulation theory, the magnetic flux is measured by the probes when the plasma column expelled from the interelectrode space passes through the frame. The following discussions were made by analyzing the shape and specific characteristics of the magnetic field signals shown in Figure 4. As can be seen, the magnetic field signals are damped signals and are composed of two half-periods. Also, it can be observed that the signals of the opposite probes oscillate in anti-phases ( $B_{\varphi=0}$  and  $B_{\varphi=90^\circ}$ ,  $B_{\varphi=180}$  and  $B_{\varphi=270}$ ). Furthermore, the amplitude of the  $B_{\varphi=0}$  and  $B_{\varphi=90}$  signals is two times higher than the amplitude of the  $B_{\varphi=180}$  and  $B_{\varphi=270}$  signals.

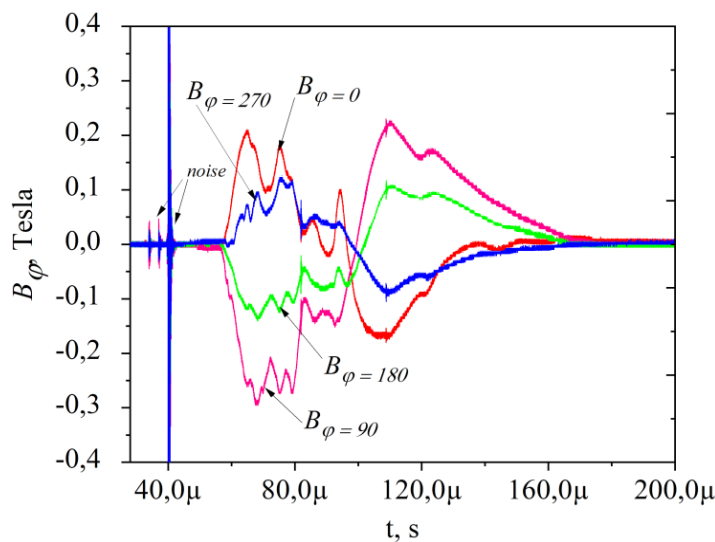


**Figure 4** – The waveforms of the plasma column azimuthal magnetic field.  $U = 4 \text{ kV}$ ,  $p = 40 \text{ mTorr}$

The obtained results are directly related to the evolution and dynamics of the plasma column. Asymmetry of the amplitude of the probe signals is explained by the asymmetry of the primary discharge formation between the electrodes. Dividing the cross section of the electrode system into four sectors, it can be concluded from the obtained results that the discharge is mainly concentrated in the top and right sector compared to the other

sectors. The following illustration is considered for a more detailed discussion of this explanation (Figure 5). The discharge current oscillogram has three half-periods (Figure 3) where two of which are positive and one is negative. This indicates that the polarity signs of the inner and outer electrodes are reversed. Thus, the evolution and dynamics of the plasma column in the accelerator channel will be as shown in Figure 5.

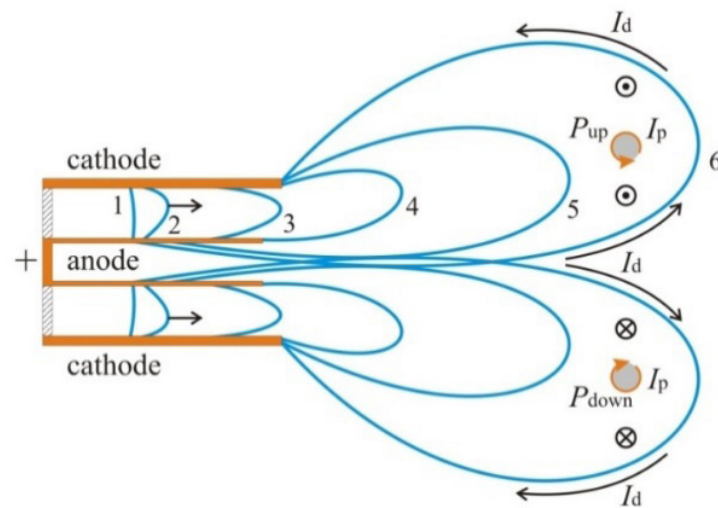


**Figure 5** – The plasma column magnetic field generation mechanism in the first half of the period

After the stored electrical energy in the capacitor battery is transferred to the electrodes, the working gas filling the interelectrode gap is ionized and a plasma jumper is formed (1). It attaches the electrodes and shorts the external circuit of the accelerator. From this moment, the Rogowski coil starts to record the discharge current oscillation in the circuit. Current is mainly directed radially from the anode to the cathode and the magnetic field of the plasma acts on it which leads to the appearance of Ampere's Force. The Ampere's force accelerates the plasma along the axis of the electrode system (2). The Ampere's force acts on the plasma during  $\sim 10 \mu\text{s}$  while the discharge current achieves its maximum value (Figure 3). As a result, the expansion of the plasma has a parabolic shape (6) to the open end of the accelerator. In Figure 5, the cross sections of the two magnetic probes  $P_{\text{up}}$  and  $P_{\text{down}}$  are shown. Also the plasma column current lines (solid blue line) are schematically illustrated in Figure 5 and correspond to the first half-period of discharge current ( $I_d$ ) when the anode is positive and the cathode is negative. The frame illustrating the axial cross section of the coaxial electrode system is considered. The reason of oscillation in opposite phase of the two opposite magnetic probes signals can be explained by the first half-period, during of which the plasma column creates a magnetic field in space. The magnetic induction vector at the magnetic probe position  $P_{\text{up}}$  is directed toward the viewer. The magnetic induction vector is directed in the opposite direction (away from the viewer) in the case of the magnetic probe  $P_{\text{down}}$ . Therefore, the signals measured by the two probes oscillate in the opposite phase and continue in subsequent half-

periods. In subsequent half-period, the amplitude of the magnetic probe signals decreases due to the discharge current decreasing in the external circuit. Moreover, two peaks of the magnetic field are observed on the oscillograms. The magnetic field becomes weaker when the discharge current decreases slowly from its maximum value. Then the magnetic field increases while the discharge current equals zero and it can be indicated the detachment of the plasma column and transformation into the plasma flux. The magnetic probes should not detect a signal when the plasma column current is zero ( $\sim 38 \mu\text{s}$ ). In this case, the current occurs only due to the plasma flux. In addition, this can be related to the formation of the plasma column into a plasmoid shape.

The following experiment was conducted to confirm the interpretation of our results. In this experiment, in order to force the plasma flow inside the probe system, thereby limiting the escape of plasma particles to the grounded chamber wall, we used a dielectric (quartz) tube, as shown in Figure 6. This allowed more appropriate interpretation of the obtained results. In other words, by comparing the obtained oscillograms from the magnetic probes, which are shown in Figures 4 (without a tube) and 7 (with a tube), we could obtain confirming data on the structure of the plasma column.

It should be noted that in this experiment the magnetic probes were placed as in previous experiments. The waveforms of the four magnetic probes signals are shown in Figure 7. As can be seen from these waveforms, the phases of the signals in this case are the same.

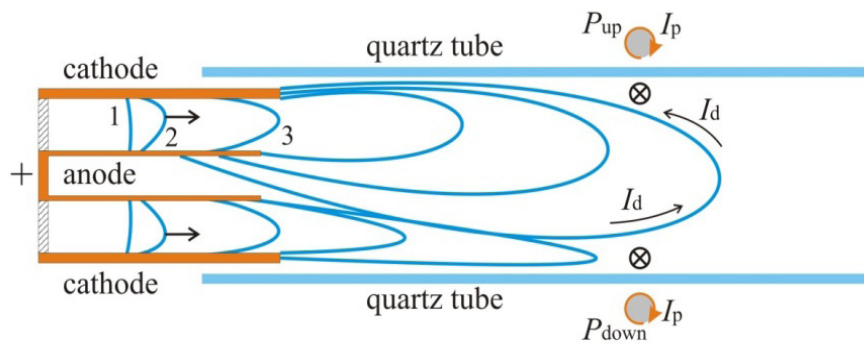


**Figure 6** – Mechanism of formation of the magnetic field of the plasma column inside the dielectric tube in the first half of the period

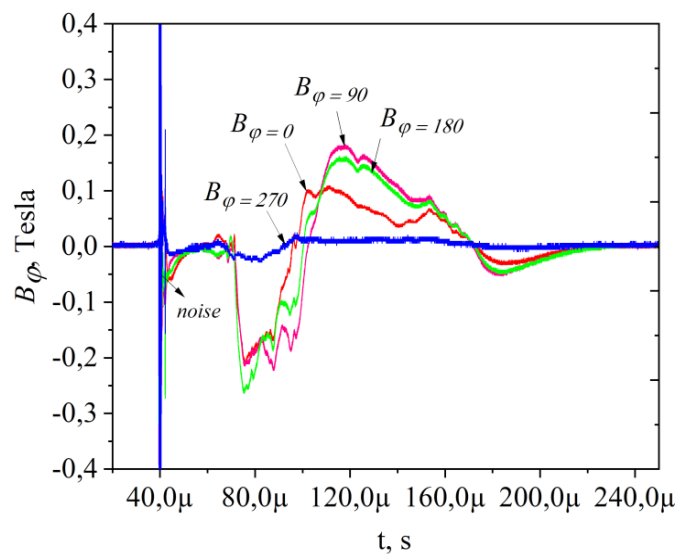


**Figure 7** – The waveforms of the plasma column azimuthal magnetic field.  $U = 3 \text{ kV}$ ,  $p = 20 \text{ mTorr}$

To clarify our observations, we can refer to Figure 6 where the plasma column current lines surrounded by a dielectric tube. The experimental results shown in Figure 6 would not have been obtained without the tube. In that case, the plasma column magnetic induction vector is directed away from us at the two points where the magnetic probes  $P_{up}$  and  $P_{down}$  are placed.

Studies on the interaction of plasma flows with candidate fusion reactor materials require the production of highly concentrated plasma fluxes on the surface. Obtaining such fluxes depends on many factors, one of which is due to the magnetic self-isolation of the plasma. In this regard, the obtained results can further be valuable in determining the optimal accelerator parameters, at which it is possible to obtain highly concentrated plasma fluxes.

The results of the plasma column azimuthal magnetic field distribution well describe the plasma flux dynamics in accelerators. The ambiguities of the configuration of the plasma column current line can be concluded from these results. In addition, the configuration of the current affects the configuration of the magnetic field. For example, it was observed that the dielectric tube changes the configuration of the plasma column current lines and also magnetic field.

#### 4 Conclusions

Such important parameters of the plasma column as the discharge current value and distribution of the azimuthal magnetic field were experimentally investigated. In addition, the plasma column



evolution and dynamics in the accelerating channel of the PW-7 coaxial plasma accelerator were studied. The experiments were conducted in two conditions. In the first case, the plasma column evolution and dynamics were studied without the dielectric (quartz) tube. In the second case the dielectric tube was used. The dielectric tube allowed avoiding plasma flux around the magnetic probes. It also avoided the plasma diffusion to the grounded wall of the chamber.

It was found that the oscillation of the magnetic probes signals occurs in anti-phase

in the first case. In the second case the plasma column current lines are changed when the column is surrounded by a dielectric tube. Therefore, the configuration of the magnetic flux of the plasma column also changes.

### Acknowledgments

This work was supported by the Ministry of Education and Science of the Republic of Kazakhstan (project no. IRN AP09259081).

### References

1. Wang, Z., Eun, Y., Wu, X. Design and demonstration of a micro air-fed magnetoplasmadynamic thruster for small satellites // *Acta Astronautica*. -2021.-Vol. 181. -P. 482-491. <https://doi.org/10.1016/j.actaastro.2021.01.047>
2. Chodun, R., Nowakowska-Langier, K., Zdunek, K., Konarski P. Characteristic STATE of substrate and coatings interface formed by impulse plasma deposition method // *Thin Solid Films*. -2018. -Vol. 663. -P. 25-30. <https://doi.org/10.1016/j.tsf.2018.08.009>
3. Bakaeva A., Makhlai V., Terentyev D., Zinoveva A., Herashchenko S., Dubinko A. Correlation of hardness and surface microcracking in ITER specification tungsten exposed at QSPA Kh-50 // *Journal of Nuclear Materials*. -2019. -Vol. 520. -P.185-192. <https://doi.org/10.1016/j.jnucmat.2019.04.008>
4. Garkusha I.E., Makhlai, V.A., Aksenov, N.N., Bazylev, B., Landman, I., Sadowski M., Skladnik-Sadowska E. Tungsten melt losses under QSPA Kh-50 plasma exposures simulating ITER ELMs and disruptions // *Fusion Science and Technology*. -2014, -Vol.65. -P. 186-193. <https://doi.org/10.13182/FST13-668>
5. Dosbolayev M.K., Tazhen A.B., Ramazanov T.S., Ussenov Ye.A. Investigation of dust formation during changes in the structural and surface properties of plasma-irradiated materials // *Nuclear Materials and Energy*. -2022. -Vol.33. -P. 101300. <https://doi.org/10.1016/j.nme.2022.101300>
6. Dosbolayev M.K., Utegenov A.U., Tazhen A.B., Ramazanov T.S. Investigation of dust formation in fusion reactors by pulsed plasma accelerator // *Laser Particle Beams*. -2017. -Vol. 35. -P. 741-749. <https://doi.org/10.1017/S0263034617000805>
7. Fortuna-Zalesn E., Grzonka J., Rubel M., Garcia-Carrasco A., Widdowson A., Baron-Wiechec A., Ciupinski L. Studies of dust from JET with the ITER-Like Wall: Composition and internal structure // *Nuclear Materials and Energy*. -2017. -Vol. 12. -P. 582-587. <https://doi.org/10.1016/j.nme.2016.11.027>
8. Smirnov R.D., Krashennnikov S.I., Pigarov A.Yu, Rognlien T.D. Tungsten dust impact on ITER-like plasma edge // *Physics of Plasmas*. -2015. -Vol.22. -P. 012506. <https://doi.org/10.1063/1.4905704>
9. Sizyuk V., Hassanein A. Potential design problems for ITER fusion device // *Sci. Rep*. -2021. -Vol.11. -P. 1-11. <https://doi.org/10.1038/s41598-021-81510-2>
10. Rabinski M., Chodun R., Nowakowska-Langier K., Zdunek K. Computational modelling of discharges within the impulse plasma deposition accelerator with a gas valve // *Physica Scripta*. -2014. -Vol. 2014. -No. T161. -P. 014049. <https://doi.org/10.1088/0031-8949/2014/T161/014049>
11. Tazhen A., Dosbolayev M., Ramazanov T. Investigation of self-generated magnetic field and dynamics of a pulsed plasma flow // *Plasma Science and Technology*. -2022. -Vol. 24. – P. 055403. <https://doi.org/10.1088/2058-6272/ac5018>
12. Underwood T.C., Subramaniam V., Riedel W.M., Raja L.L., Cappelli M.A. Effects of flow collisionality on ELM replication in plasma guns // *Fusion Engineering and Design*. -2019. -Vol. 144. -P. 97-106. <https://doi.org/10.1016/j.fusengdes.2019.04.088>
13. Brushlinskii K.V., Stepin E.V. Numerical model of compression plasma flows in channels under a longitudinal magnetic field // *Differential Equations*. -2019. -Vol. 55. -P. 929-939. <https://doi.org/10.1134/S0012266119070036>
14. Kozlov A.N., Klimov N.S., Konovalov V.S., Podkovyrov V.L., Urlova R.V. Study of the ionizing gas flow in the channel of plasma accelerator with different ways of gas inflow at the inlet // *Journal of Physics: Conference Series*. -2019. -Vol. 1394. -P. 012021. <https://doi.org/10.1088/1742-6596/1394/1/012021>

15. Beresnyak A., Giuliani J.L., Jackson S.L., Richardson A.S., Swanekamp S., Schumer J., Weber B., Mosher D. Simulations of a dense plasma focus on a high-impedance generator // *IEEE Transactions on plasma science*. -2018. -Vol.46. -P. 3881-3885. <https://doi.org/10.1109/TPS.2018.2865188>
16. Saw S.H., Akel M., Lee P.C.K., Ong S.T., Mohamad S.N., Ismail F.D., Nawi N.D., Devi K., Sabri R.M., Baijan A.H., Ali J., Lee S. Magnetic probe measurements in INTI plasma focus to determine dependence of axial speed with pressure in neon // *Journal of Fusion Energy*. -2012. -Vol. 31. -P. 1-6. <https://doi.org/10.1007/s10894-011-9487-z>
17. Piriaei D., Javadi S., Mahabadi T.D., Yousefi H.R., Salar Elahi A. Ghoranneviss M. The influence of the cathode array and the pressure variations on the current sheath dynamics of a small plasma focus device in the presence of an axial magnetic probe // *Physics of Plasmas*. -2017. -Vol. 24. -P. 043504. <https://doi.org/10.1063/1.4979275>
18. Tazhen A.B., Dosbolayev M.K. Measuring the self-generated magnetic field and the velocity of plasma flow in a pulsed plasma accelerator // *Recent Contributions to Physics*. -2021. -Vol. 77. -P. 30-39. <https://doi.org/10.26577/10.26577/RCPH.2021.v77.i2.04>
19. Krauz V.I., Mitrofanov K.N., Kharrasov A.M., Il'ichev I.V., Myalton V.V., Anan'ev S.S., Beskin V.S. Laboratory modeling of the rotation of jets ejected from young stellar objects at studies the azimuthal structure of an axial jet at the PF-3 facility // *Astronomy Reports*. – 2021. -Vol. 65. -P. 26-44. <https://doi.org/10.1134/S1063772921010029>
20. Dosbolayev M.K., Tazhen A.B., Ramazanov T.S. Investigation and diagnostics of plasma flows in a pulsed plasma accelerator for experimental modeling of processes in tokamaks // *Eurasian Journal of Physics and Functional Materials*. -2021. -Vol. 5. -P. 198-210. <https://doi.org/10.32523/ejpfm.2021050404>
21. Dosbolayev M.K., Tazhen A.B., Ramazanov T.S. Method and apparatus for measuring the spatio-temporal distribution of magnetic field of a pulsed plasma flow. Patent № 35200 Republic of Kazakhstan. 03.12.2021, – 5 p.
22. Karimi F.S., Saviz S., Ghoranneviss M., Salem M.K., Aghamir F.M. The circuit parameters measurement of the SABALAN-I plasma focus facility and comparison with Lee model // *Results in Physics*. -2017. -Vol. 7. -P. 1859-1869. <https://doi.org/10.1016/j.rinp.2017.05.021>